

1-P

# NASA TECHNICAL MEMORANDUM

NASA TM X-64730

## EVALUATION OF FLEXIBLE RING BAFFLES FOR DAMPING LIQUID OSCILLATIONS

By Frank Bugg  
Aero-Astroynamics Laboratory

January 12, 1973



**NASA**

*George C. Marshall Space Flight Center  
Marshall Space Flight Center, Alabama*

(NASA-TM-X-64730) EVALUATION OF FLEXIBLE  
RING BAFFLES FOR DAMPING LIQUID  
OSCILLATIONS (NASA) 34 p HC \$3.75

N73-21273

CSSL 20D

Unclas  
67980

G3/12

1. REPORT NO. TM X-64730		2. GOVERNMENT ACCESSION NO.		3. RECIPIENT'S CATALOG NO.	
4. TITLE AND SUBTITLE Evaluation of Flexible Ring Baffles for Damping Liquid Oscillations				5. REPORT DATE January 12, 1973	
				6. PERFORMING ORGANIZATION CODE 7722	
7. AUTHOR(S) Frank Bugg				8. PERFORMING ORGANIZATION REPORT #	
9. PERFORMING ORGANIZATION NAME AND ADDRESS George C. Marshall Space Flight Center Marshall Space Flight Center, Alabama 35812				10. WORK UNIT NO.	
				11. CONTRACT OR GRANT NO.	
12. SPONSORING AGENCY NAME AND ADDRESS National Aeronautics and Space Administration Washington, D.C. 20546				13. TYPE OF REPORT & PERIOD COVERED Technical Memorandum	
				14. SPONSORING AGENCY CODE	
15. SUPPLEMENTARY NOTES Prepared by Aero-Astroynamics Laboratory, Science and Engineering					
16. ABSTRACT  An experimental study was undertaken of damping produced by single flexible-ring baffles in a 396-cm diameter tank of liquid nitrogen. Two 24.8-cm wide baffles were tested. One baffle was 0.00635 cm thick type 301 stainless steel and the other 0.0254 cm thick Teflon FEP. Each baffle produced damping of liquid oscillations equal to or greater than that expected from rigid baffles of the same size. The equations used to determine the baffle thickness required were found to be adequate baffle design equations.					
17. KEY WORDS slosh damping flexible baffles			18. DISTRIBUTION STATEMENT Unclassified - unlimited <i>E. D. Geissler</i> E. D. Geissler Director, Aero-Astroynamics Laboratory		
19. SECURITY CLASSIF. (of this report) Unclassified		20. SECURITY CLASSIF. (of this page) Unclassified		21. NO. OF PAGES 34	22. PRICE NTIS

TABLE OF CONTENTS

	Page
SUMMARY .....	1
INTRODUCTION.....	1
APPARATUS.....	2
Test Equipment .....	2
Baffles.....	4
PROCEDURE.....	8
Test.....	8
Data Reduction.....	8
DISCUSSION OF RESULTS.....	11
Damping and Frequency.....	11
Strength and Weight .....	25
CONCLUSIONS.....	26
REFERENCES.....	27

Preceding page blank

## LIST OF ILLUSTRATIONS

Figure	Title	Page
1.	Tank and excitation mechanism. . . . .	3
2.	Schematic of tank interior . . . . .	4
3.	Steel baffle . . . . .	6
4.	Baffle installation. . . . .	7
5.	Typical amplitude decay records. . . . .	10
6.	Amplitude versus cycle number . . . . .	12
7.	Effect of baffle location on slosh frequency . . . . .	12
8.	Effect of steel baffle depth on damping . . . . .	13
9.	Effect of Teflon baffle depth on damping . . . . .	18
10.	Effect of slosh amplitude on damping . . . . .	21
11.	Effect of period parameter on relative damping . . . . .	23

## LIST OF TABLES

Table	Title	Page
1.	Experimental Data . . . . .	9
2.	Calculated Data . . . . .	17

## DEFINITIONS OF SYMBOLS

d	Baffle depth below the liquid equilibrium free surface, cm
E	Modulus of elasticity, dynes/cm <sup>2</sup>
F	Flexibility parameter, $F = 0.04 \frac{(\rho g R)}{E} \left( \frac{W_f}{R} \right)^5 \left( \frac{R}{t} \right)^3$
g	Axial acceleration of tank-liquid system, cm/sec <sup>2</sup>
K	Factor of safety, $\sigma_y/\sigma$
n	Number of cycles
P	Period parameter, $P = \frac{2\pi\zeta}{W} e^{-1.84 (d/R)}$
p	Pressure, dynes/cm <sup>2</sup>
R	Tank radius, cm
t	Baffle thickness, cm
W	Baffle width, cm
W <sub>f</sub>	Width of flexible portion of baffle, cm
γ	Damping ratio, $\delta/2\pi$
γ <sub>f</sub>	Damping provided by flexible baffle
γ <sub>r</sub>	Theoretical damping provided by rigid baffle
δ	Log decrement of damping
ζ	Liquid oscillation amplitude, cm
ζ <sub>0</sub>	Amplitude at cycle number 0, cm

## DEFINITIONS OF SYMBOLS (Concluded)

$\zeta_n$	Amplitude at cycle number n, cm
$\zeta_{\max}$	Maximum amplitude, cm
$\rho$	Liquid density, gm/cm <sup>3</sup>
$\rho_B$	Baffle material density, gm/cm <sup>3</sup>
$\sigma$	Tensile stress in baffle material, dynes/cm <sup>2</sup>
$\sigma_y$	Yield strength in tension of baffle material, dynes/cm <sup>2</sup>
$\omega$	Oscillation frequency, Hz

## EVALUATION OF FLEXIBLE RING BAFFLES FOR DAMPING LIQUID OSCILLATIONS

### SUMMARY

An experimental study was undertaken of damping produced by single flexible-ring baffles in a 396-cm diameter tank of liquid nitrogen. Two 24.8-cm wide baffles were tested. One baffle was 0.00635-cm thick type 301 stainless steel, and the other 0.0254-cm thick Teflon FEP.\* Each baffle produced damping of liquid oscillations equal to or greater than that expected from rigid baffles of the same size. The equations used to determine the flexible baffle thickness required were found to be adequate baffle-design equations.

### INTRODUCTION

Ring baffles have been used successfully as slosh-suppression devices in the liquid propellant tanks of several launch vehicle stages. Ring baffles were chosen because studies such as Reference 1 showed that they gave greater propellant control for less baffle area than other baffle configurations. Experimental investigations such as References 2 and 3 indicate that the average damping provided by flexible ring baffles is greater than that from equal-size rigid rings. If rigidity is no longer a requirement, baffles can be made much lighter; therefore, significant reduction in slosh suppression system weight should be realized. The next generation of space vehicles, the Shuttle and its various payloads, the Tug, and other planned or proposed liquid-containing spacecraft, can be designed to use flexible baffles if the advantages hold for slosh suppression in large tanks and in cryogenic liquid.

The investigation reported in Reference 4 considered several candidate flexible baffle materials and developed design equations for sizing flexible baffles based on damping required, amplitude expected, baffle depth, and material strength. Damping tests in a small tank showed that several

---

\*Trade name of E.I. Dupont de Nemours and Co. for a fluorinated ethylene propylene film.

materials were still flexible and performed well in liquid nitrogen. Two materials, Teflon FEP and type 301 stainless steel, were chosen as least likely to react with oxygen and subjected to fatigue tests in liquid oxygen as reported in Reference 5. The tests simulated mechanical, thermal, and chemical stresses that materials would experience as baffles in a reusable liquid oxygen tank. No deterioration of the test specimens was found.

The purpose of the present investigation was to test the flexible baffle advantages in a large scale tank of cryogenic liquid and to verify the adequacy of design equations developed in Reference 4. To accomplish this purpose, an experimental investigation was made of damping produced by flexible baffles in a 3.96-m diameter tank of liquid nitrogen. The baffles, one made of Teflon FEP and the other of type 301 stainless steel, were sized using the design equations of Reference 4. The baffle width was chosen as 0.125 times the tank radius. The baffles were tested at liquid depths from 0 to 0.3 radius and at slosh amplitudes up to 0.37 radius.

## APPARATUS

### Test Equipment

The test tank and excitation mechanism are shown in Figure 1. The desired excitation frequency was produced by a variable-speed hydraulic drive system. The drive system turned a crankshaft which moved the rocking block. The top of the block moved several inches horizontally while the lower end had essentially zero horizontal motion. The turnbuckles raised or lowered the block relative to its attachment point to the yoke and in this way the horizontal amplitude of the tank was adjusted. The output from a potentiometer-type displacement transducer attached to the yoke and to an I-beam of the test stand gave tank position as a function of time. The tank was suspended by three vertical parallel arms (one on either side and one behind the tank as viewed in Figure 1) pinned to the tank and pinned to the test stand. The inside dimensions of the tank are shown in Figure 2.

The test liquid was nitrogen. It was chosen because its viscosity, density, and temperature are close to those of liquid oxygen (a likely-to-be-baffled propellant) and because of its chemical inertness. The nitrogen kinematic viscosity was  $0.0021 \text{ cm}^2/\text{sec}$ , the density  $0.815 \text{ gm/cm}^3$ , and the temperature  $-198^\circ\text{C}$ . A capacitance-type liquid-level probe, located as shown in Figure 2, was used to measure the liquid level and slosh amplitude. An oscillograph was used to record the outputs of the tank displacement potentiometer and the liquid level probe.

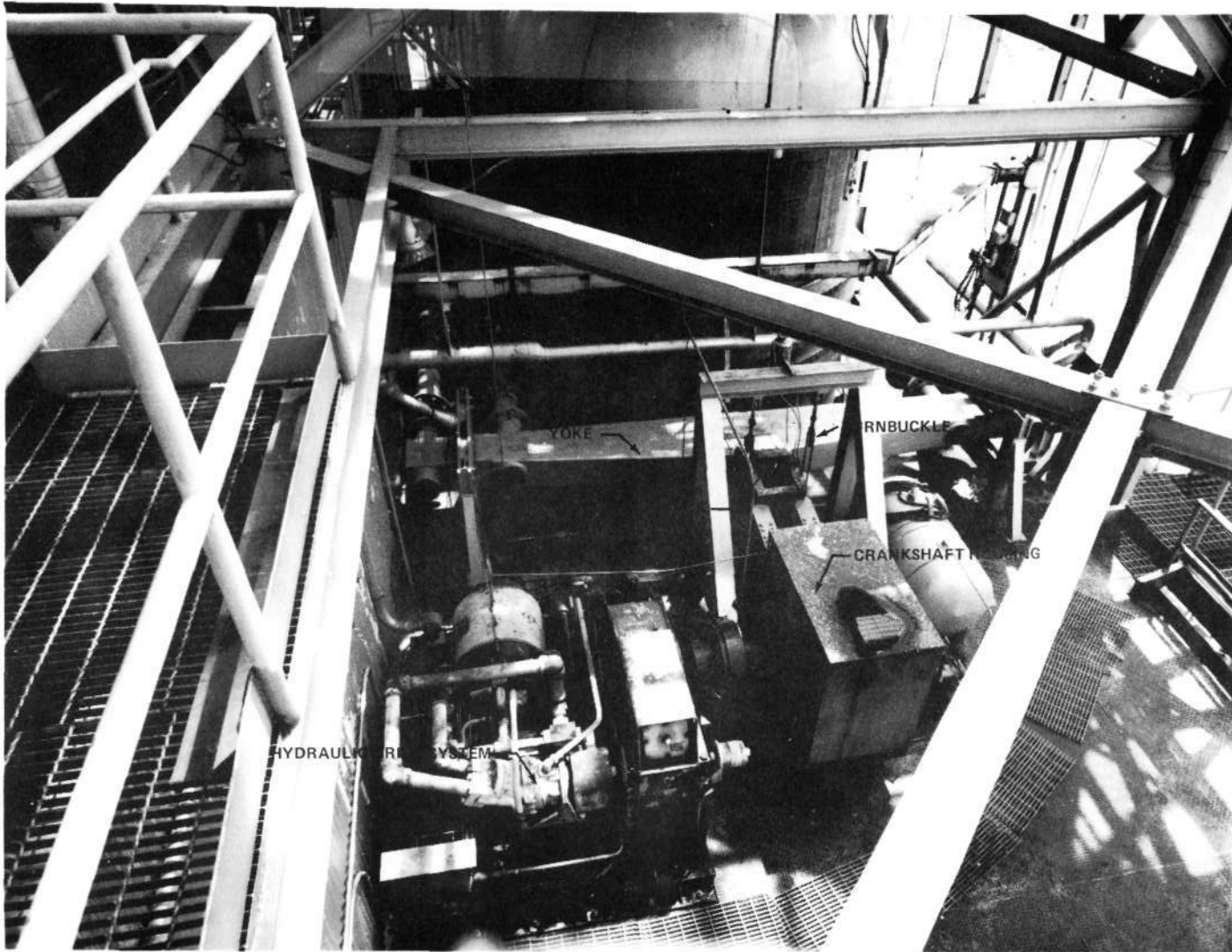


Figure 1. Tank and excitation mechanism.

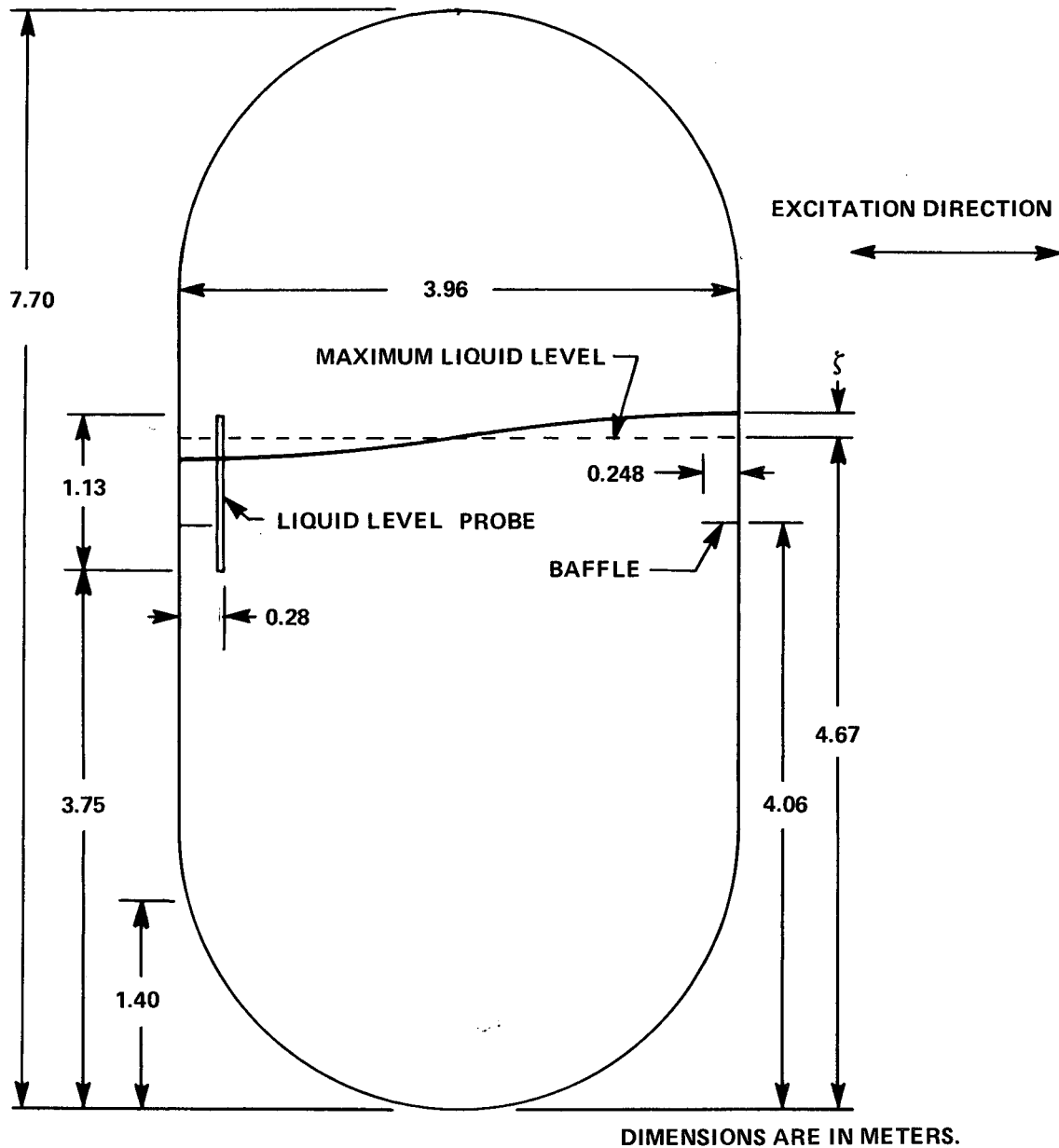


Figure 2. Schematic of tank interior.

## Baffles

Materials. Properties of the two baffle materials used are shown in the following:

Material	$\rho, \frac{\text{gm}}{\text{cm}^3}$	t, cm	20° C		-198° C	
			$\sigma_y, \frac{\text{dynes}}{\text{cm}^2}$	E, $\frac{\text{dynes}}{\text{cm}^2}$	$\sigma_y, \frac{\text{dynes}}{\text{cm}^2}$	E, $\frac{\text{dynes}}{\text{cm}^2}$
Teflon FEP	2.15	0.0254	$8.49 \times 10^7$	$0.7 \times 10^{10}$	$88.6 \times 10^7$	$7.2 \times 10^{10}$
Type 301 Stainless Steel	7.85	0.00635	$904 \times 10^7$	$207 \times 10^{10}$	$1008 \times 10^7$	$207 \times 10^{10}$

These were taken from References 4 and 5. Several plastics, including Teflon FEP, were examined as reported in Reference 4 and found to be suitable flexible baffle materials for use in cryogenic liquids. Teflon FEP was selected from the plastics for the large scale tests because of its relative insensitivity to reaction with oxygen. The analysis of Reference 4 also indicated that high tensile strength materials would provide flexibility and light weight, and on this basis, the high strength stainless steel was chosen.

Design. The baffle-width parameter,  $W/R = 0.125$ , was chosen as representative of baffle widths used in production vehicles and as a convenient size for use in the available test facility. The following equations from Reference 4,

$$t = 0.57 R \left( \frac{W}{R} \right)^{\frac{1}{2}} \left( \frac{K^{\frac{3}{2}} E^{\frac{1}{2}} P}{\sigma_y^{\frac{3}{2}}} \right) \quad (1)$$

$$P = 5.9 \rho g R \left( \frac{W}{R} \right)^{0.485} \left( \frac{\zeta}{R} \right)^{1.515} e^{-2.79 \left( \frac{d}{R} \right)} \quad (2)$$

were used to determine the baffle thickness required for each material. In Reference 4, a factor of safety  $K = 3$  was recommended for use in equation (1). Commercially available material thicknesses were used and the resulting safety factors were 2.5 for the Teflon and 3.6 for the steel, when the liquid amplitude was  $0.1 R$  with  $d/R = 0$ . An efficiency of 75 percent was assumed for the riveted baffle joint.

Installation. Figure 3 shows the steel baffle and the liquid-level probe installed in the tank. Figure 4 shows details of the baffle installation. The test tank had twenty T-shaped stringers mounted vertically on the tank wall. The baffle consisted of ten segments. Baffle support angles were bolted to the stringers, and the baffle segment edge was clamped between the support

Reproduced from  
best available copy.



6



Figure 3. Steel baffle.

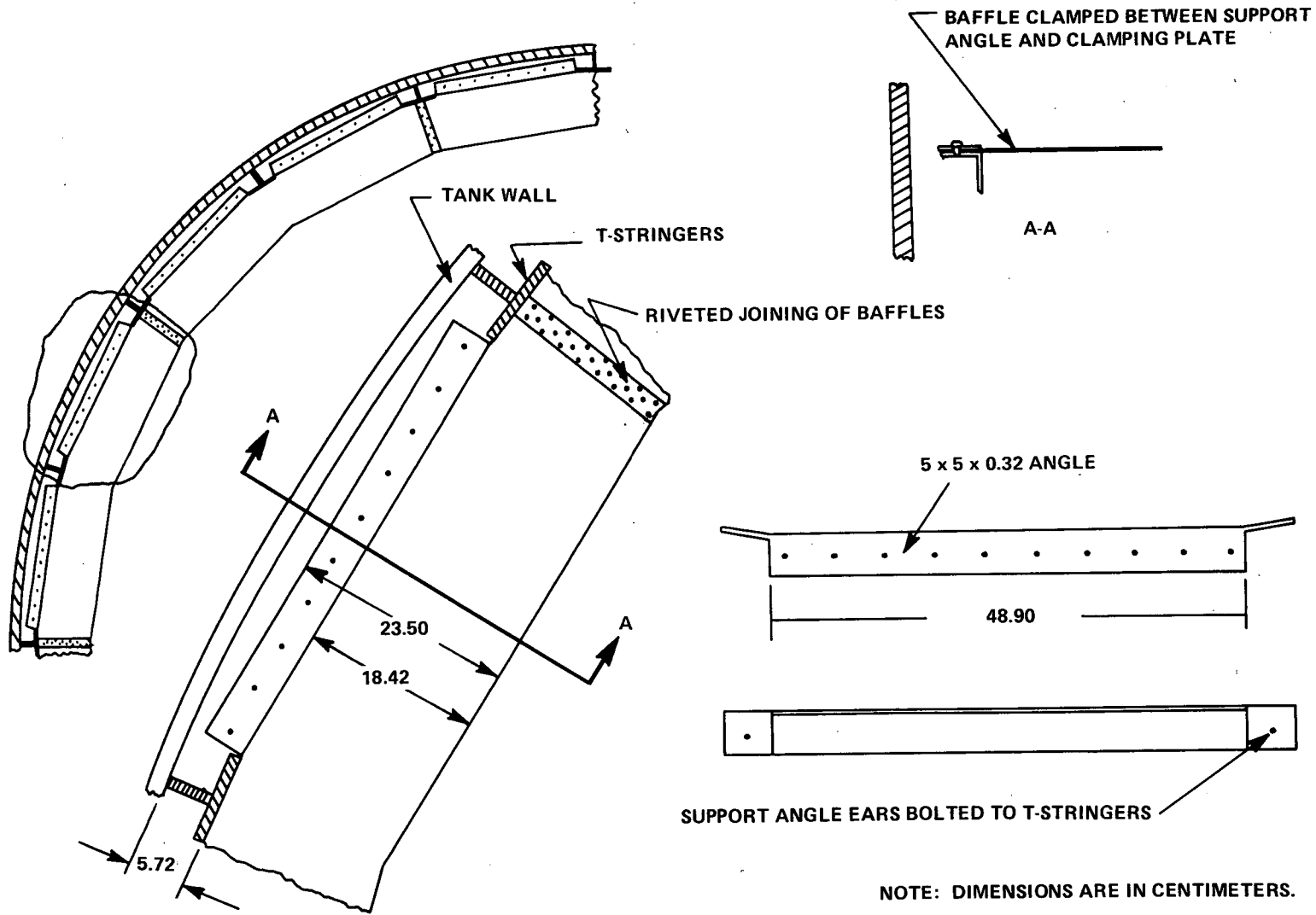


Figure 4. Baffle installation.

angle and clamping plate. After the segments were attached to the tank wall, the overlapping ends of the segments were joined to each other by riveting them between two doubler-plates. The installed steel baffle was smooth and generally wrinkle-free. There was apparently a small amount of slack in the baffle, and this caused the baffle edge toward the tank center to droop 2.5 cm below the stationary baffle edge. The installed Teflon baffle had a few more wrinkles than the steel baffle and showed about 3.0-cm droop of its unsupported edge.

## PROCEDURE

### Test

The test procedure was as follows: after installation of the steel baffle, the tank was filled to the maximum test level (the baffle was then at a depth of approximately 0.3R). With the excitation amplitude set at 6.04 cm, the hydraulic drive system was operated at an excitation frequency below the liquid natural frequency to produce a maximum liquid amplitude near 0.1R. The drive system was stopped after three or four cycles at the desired frequency. By stopping the drive, the tank was locked to the test stand and data taken during the ensuing free decay of the liquid oscillation were used to determine damping and natural frequency (the tank displacement transducer indicated less than 0.025-cm tank motion during decay). Two free decays were recorded at each level. Liquid was then drained from the tank until the next test level was reached. The values of  $d/R$  resulting for each liquid level are listed in Table 1 along with the natural frequencies and excitation frequencies.

A similar procedure was used with the Teflon baffle, except that after completing the series of baffle depths, two additional excitations and decays were performed with the baffle near the liquid surface. For these, an excitation frequency nearer the liquid natural frequency was used in order to give a slosh amplitude large enough to test the conservatism of the baffle design equations. After completion of the baffle tests, the damping was measured with the baffles and support angles removed from the tank.

### Data Reduction

Portions of two typical oscillograph traces of liquid level probe output during oscillation decay are shown in Figure 5. The liquid oscillation natural

TABLE 1. EXPERIMENTAL DATA

Material	$\frac{d}{R}$	$\gamma$ ( $\frac{\zeta}{R} = 0.02$ )	$\gamma$ ( $\frac{\zeta}{R} = 0.04$ )	$\gamma$ ( $\frac{\zeta}{R} = 0.06$ )	$\omega$ (Hz)	Tank Amplitude, cm	Excitation Frequency, Hz	$\zeta_{max}$ , cm
Steel ↓	0	0.0464	0.0491	0.0499	0.491	6.04 ↓	0.42	33.5
	0.0154	0.0892	0.0320	0.0425	0.505		↓	35.1
	0.0487	0.0589	0.0594	--	0.488		0.37	18.7
	0.0628	0.0589	0.0594	--	0.477		↓	17.8
	0.1101	0.0382	0.0440	0.0494	0.468		↓	21.3
	0.1129	0.0408	0.0411	0.0599	0.471		↓	20.7
	0.1475	0.0285	0.0363	0.0430	0.465		0.33	14.1
	0.150	0.0339	0.0341	0.0344	0.465		↓	13.3
	0.203	0.0234	0.0239	0.0256	0.466		↓	15.2
	0.205	0.0295	0.0301	--	0.464		0.25	10.2
	0.214	0.0234	0.0290	0.0370	0.468		0.33	15.2
	0.251	0.0190	0.0210	--	0.468		↓	12.6
	0.259	0.0193	0.0204	--	0.467		↓	15.9
	0.304	0.0135	0.0174	0.0223	0.470		↓	14.0
	0.307	--	0.0154	0.0260	0.469		↓	12.7
	Teflon ↓	0	0.0676	0.0578	0.0525		0.498	0.37
0.018		0.0690	0.0360	0.0517	0.504	↓	17.8	
0.0513		0.0564	0.0454	--	0.480	↓	18.2	
0.0538		0.0726	0.0560	--	0.484	↓	17.9	
0.0987		0.0419	0.0436	0.0468	0.468	↓	19.1	
0.100		0.0290	0.0381	--	0.464	↓	20.1	
0.148		0.0271	0.0328	0.0371	0.463	0.33	13.7	
0.160		0.0317	0.0336	0.0358	0.465	↓	14.4	
0.188		0.0159	0.0296	0.0433	0.468	↓	13.8	
0.199		0.0185	0.0267	0.0362	0.469	↓	13.3	
0.259		0.0164	0.0167	0.0333	0.471	↓	13.8	
0.263		0.0153	0.0200	--	0.469	↓	12.7	
0.294		--	0.0177	--	0.472	↓	15.9	
0.294		--	0.0142	0.0177	0.468	↓	13.3	
0.0128		--	0.0156	0.0141	0.471	0.43	73.4	
0.0154		--	0.0161	0.0155	0.479	↓	63.8	
None ↓	--	0.00171	0.00171	0.00171	0.476	0.33	11.4	
	--	0.00187	0.00187	0.00187	0.476	↓	15.2	

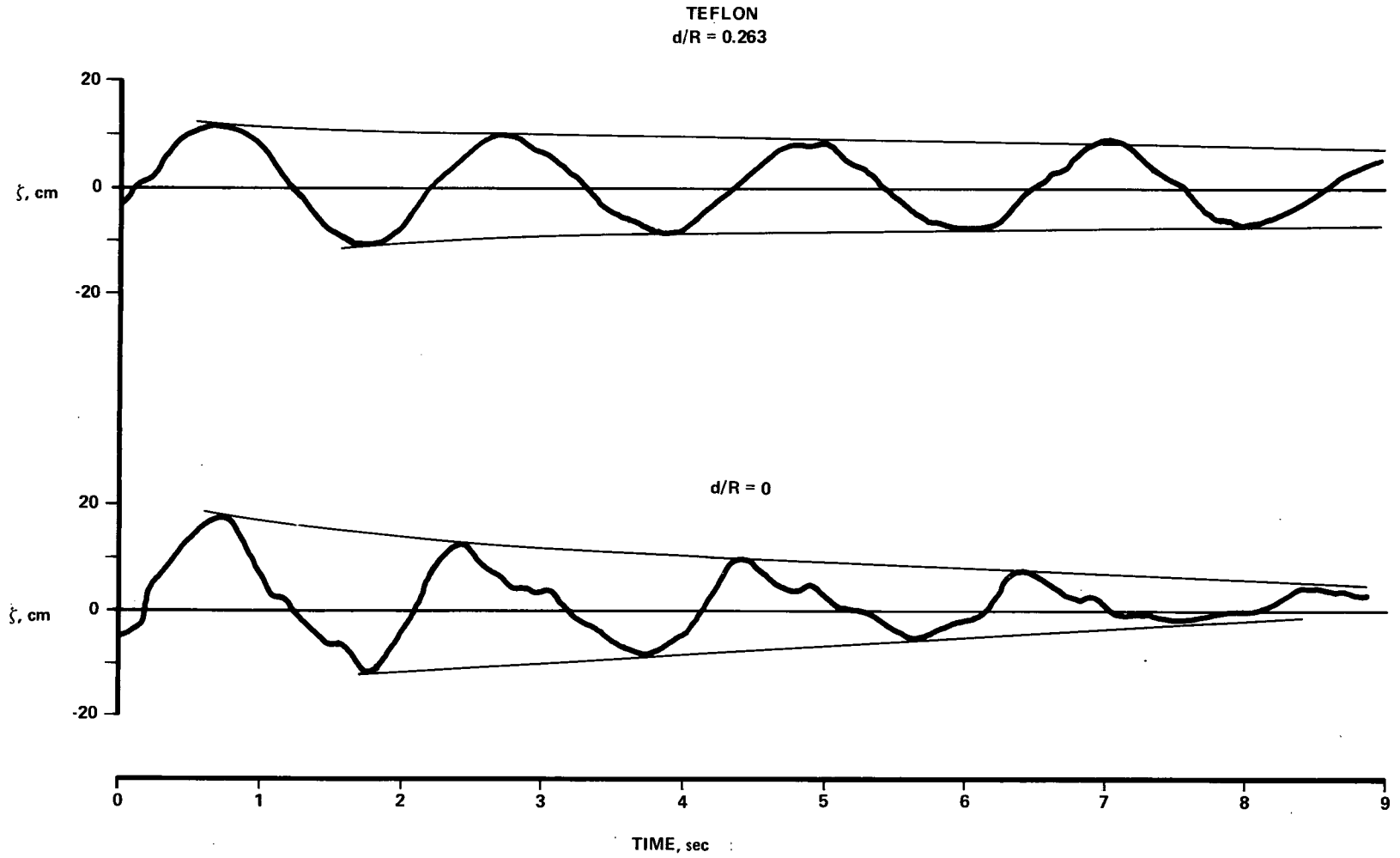


Figure 5. Typical amplitude decay records.

frequency and damping were determined by first selecting a part of the total oscillograph record starting with the first cycle which was apparently free of transients and continuing as far as the cycles were well-defined. Smooth curves were then drawn through the amplitude peaks to form envelopes of maximum amplitude. An average period of oscillation was computed for the chosen portion of record. Peak-to-peak amplitudes,  $2\zeta$ , were taken from the record at one-period intervals and plotted versus number of cycles on semi-log paper as shown in Figure 6. The slope of each curve was measured at amplitudes,  $\zeta$ , equal to  $0.02R$ ,  $0.04R$ , and  $0.06R$ . The slope is:

$$\delta = \frac{\ln 2\zeta_0 - \ln 2\zeta_n}{n}$$

which is the log decrement of damping. The damping ratio  $\gamma = \delta/2\pi$  is used to present the damping data in this report.

A summary of the damping values and frequencies is shown in Table 1.

## DISCUSSION OF RESULTS

### Damping and Frequency

Effect of Baffle Depth. The baffle depth was varied by changing the liquid level in the tank while the baffle remained in one position. The minimum liquid level was 2.05 times the tank radius. For liquid levels greater than twice the radius, changes in liquid level have a negligible effect on frequency and damping [6] compared to the effects of the baffle presence.

Figure 7 shows the change in frequency of the liquid oscillation as a function of baffle depth. From  $d/R = 0.1$  to  $0.3$ , the damped frequency is, as expected, lower than the frequency without a baffle (dashed-line, near-zero damping). The geometry of the surface is changed as the baffle depth is decreased to less than  $0.1R$  and the frequency approaches that for liquid in a tank with diameter equal to the inner-baffle diameter (dotted line,  $R = 1.73\text{-m}$ ).

The effect of baffle depth on the damping produced by the steel baffle is shown in Figure 8 for three amplitudes. The equation,

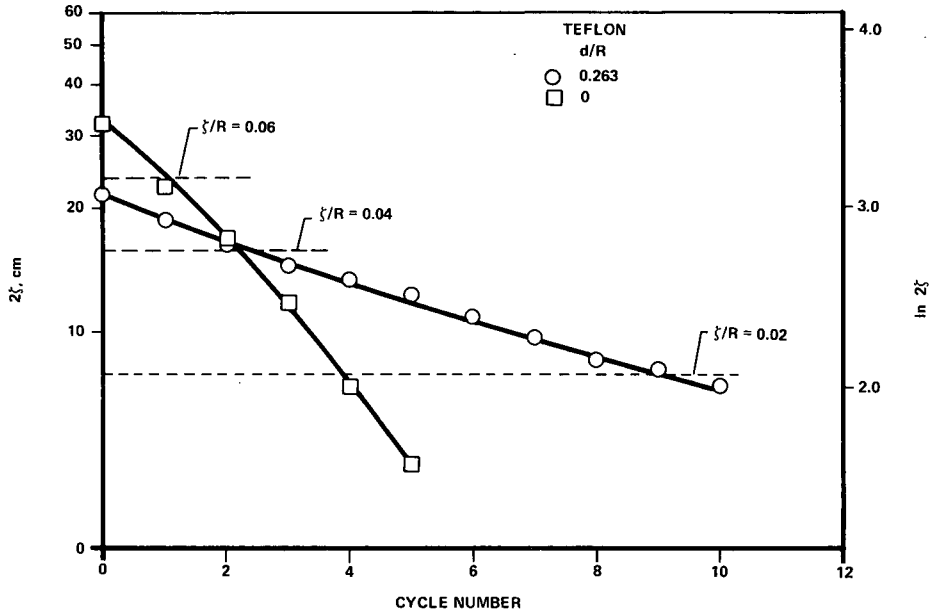


Figure 6. Amplitude versus cycle number.

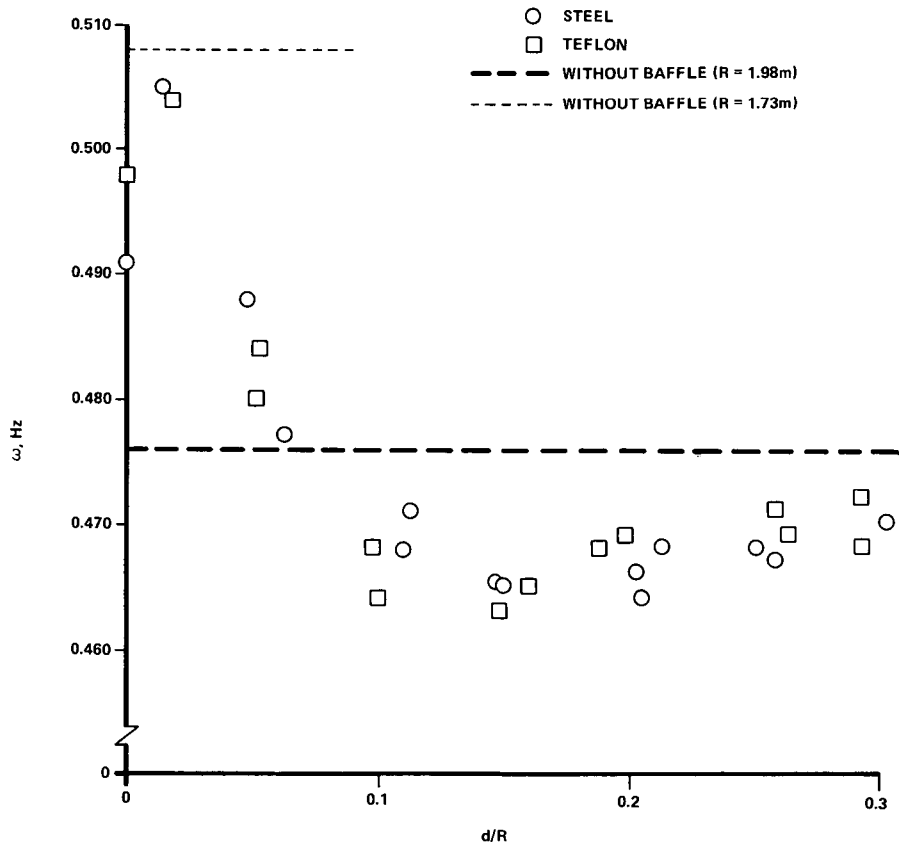
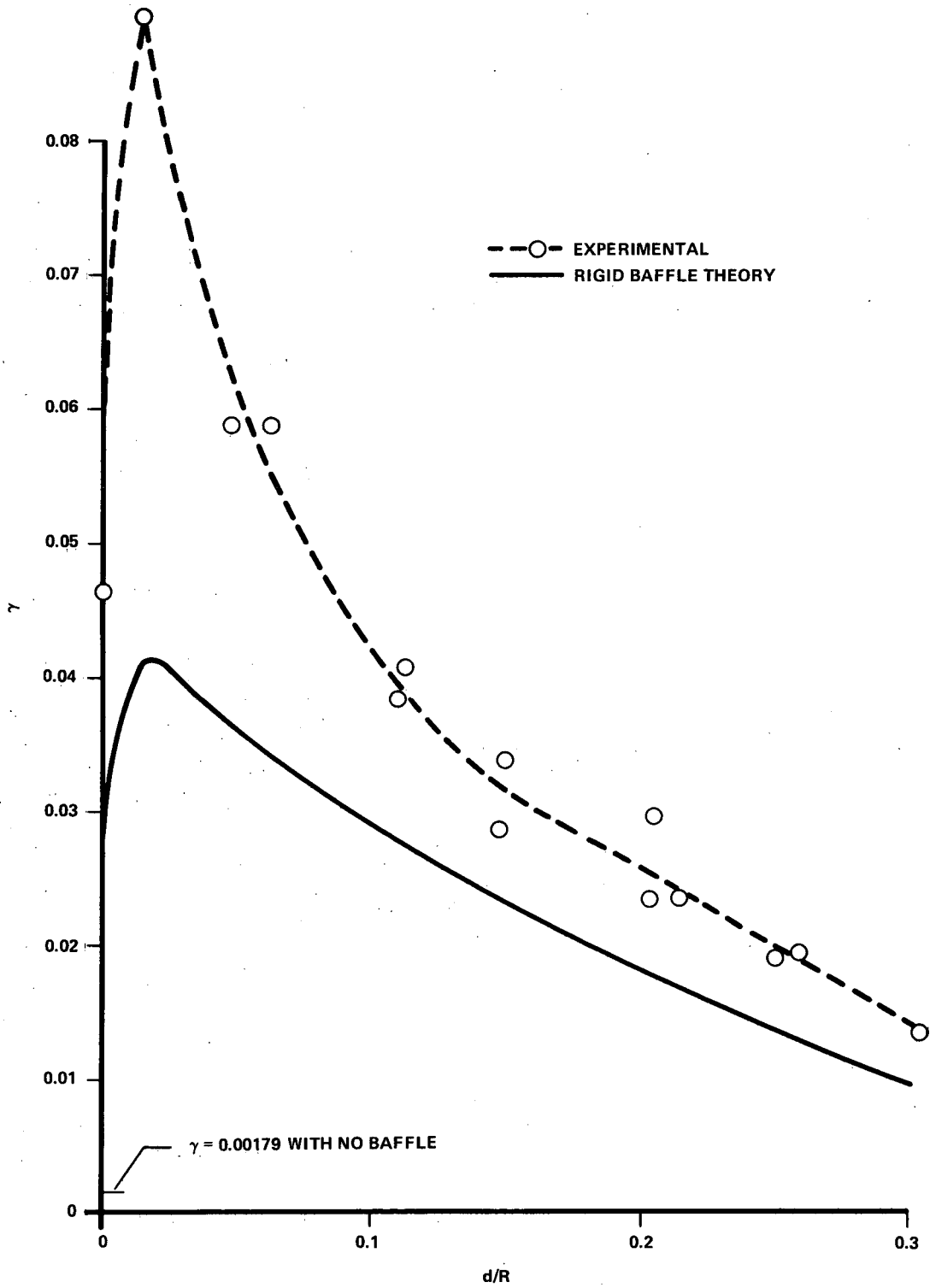
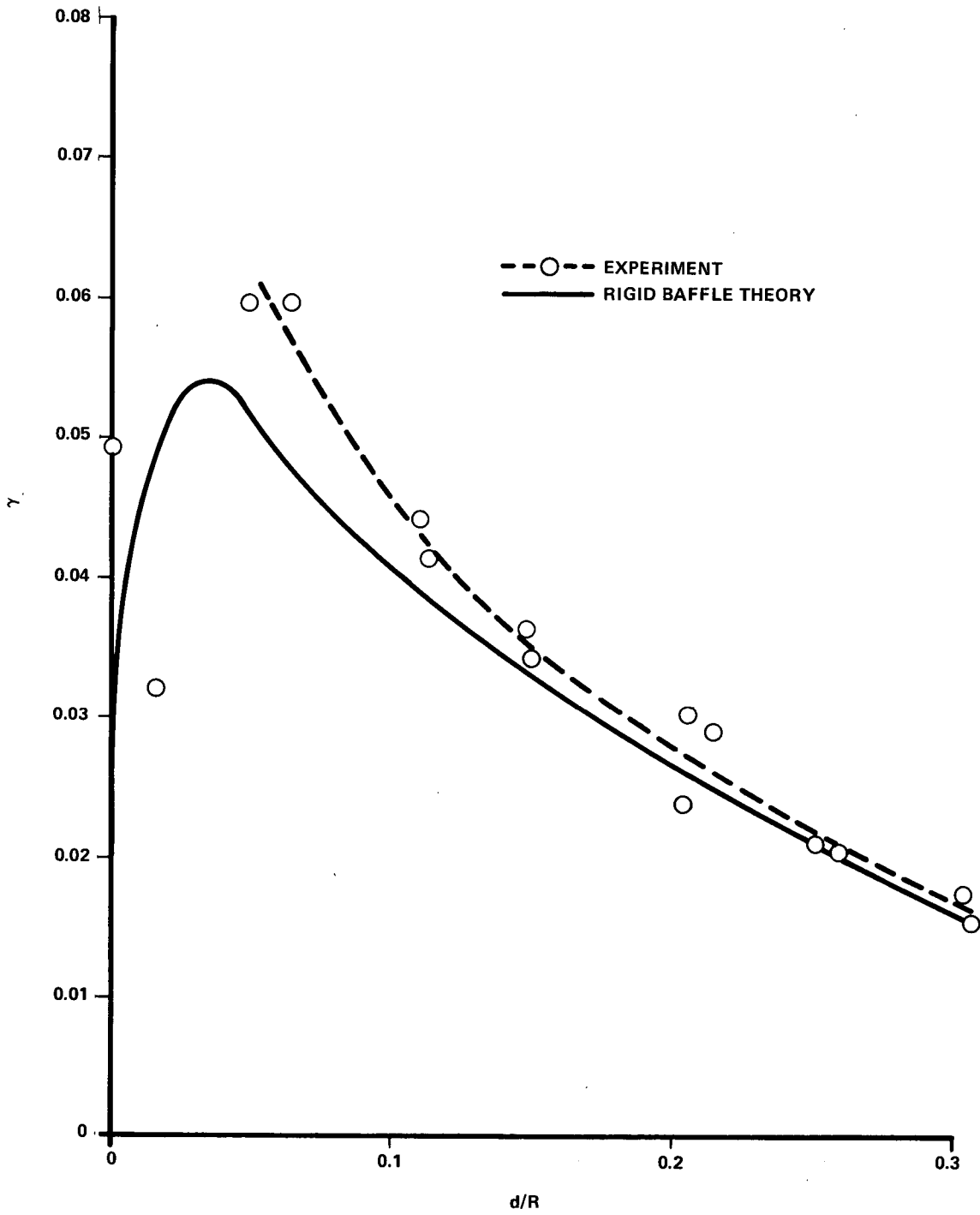


Figure 7. Effect of baffle location on slosh frequency.



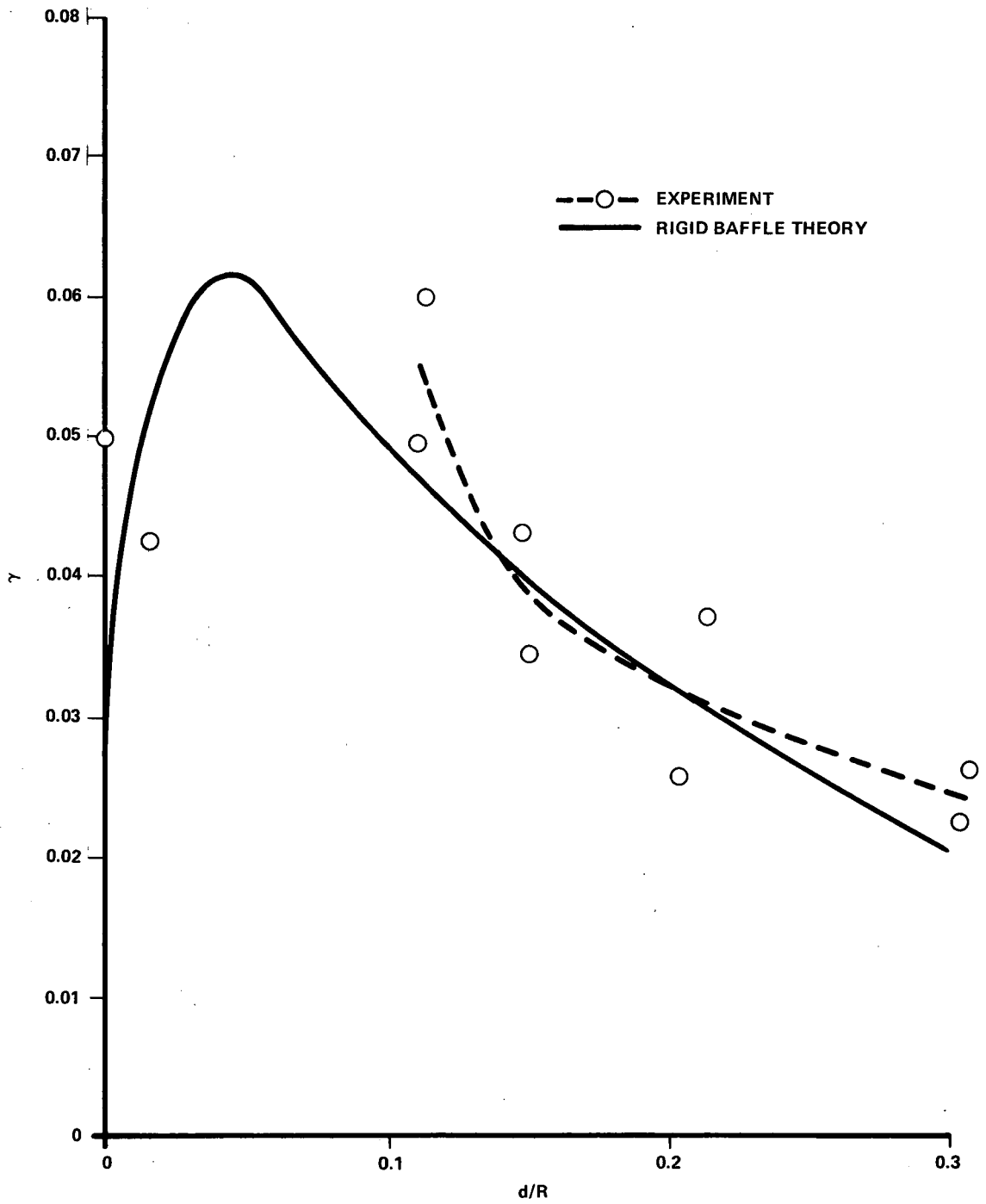
(a).  $\zeta/R = 0.02$ .

Figure 8. Effect of steel baffle depth on damping.



(b).  $\zeta/R = 0.04$ .

Figure 8. (Continued).



(c).  $\xi/R = 0.06$ .

Figure 8. (Concluded).

$$\gamma_r = 2.8 \left[ \frac{W}{R} \left( 2 - \frac{W}{R} \right) \right]^{\frac{3}{2}} \left( \frac{\zeta}{R} \right)^{\frac{1}{2}} e^{-4.6 \left( \frac{d}{R} \right)}, \quad (3)$$

from Reference 4 was used to compute the damping expected from a rigid baffle with  $W/R = 0.125$ , and the values of  $\gamma_r$  calculated at test values of  $d/R$  are shown in Table 2. The values of  $\gamma_r$  calculated at baffle depths less than the slosh amplitude were reduced as discussed in Chapter 4 of Reference 6 to account for a portion of the baffle being out of the liquid. The dashed line was drawn using average experimental values and the shape of the rigid baffle theoretical curve as guides. There was generally more scatter in the data at low baffle depth and at high amplitude (the situations for which there is the most liquid surface disturbance).

Figure 8a shows that the flexible steel baffle gave considerably more damping than predicted for a rigid baffle of the same size at all baffle depths investigated. At this amplitude,  $\zeta/R = 0.02$ , the ratio of flexible to rigid baffle damping increased from about 1.5 at  $d/R = 0.3$  to 2.18 at  $d/R = 0.15$ . The maximum damping occurs near the minimum baffle depth for which the baffle is completely submerged during the entire slosh cycle. The damping measured for the tank without baffles is shown as  $\gamma = 0.00179$ .

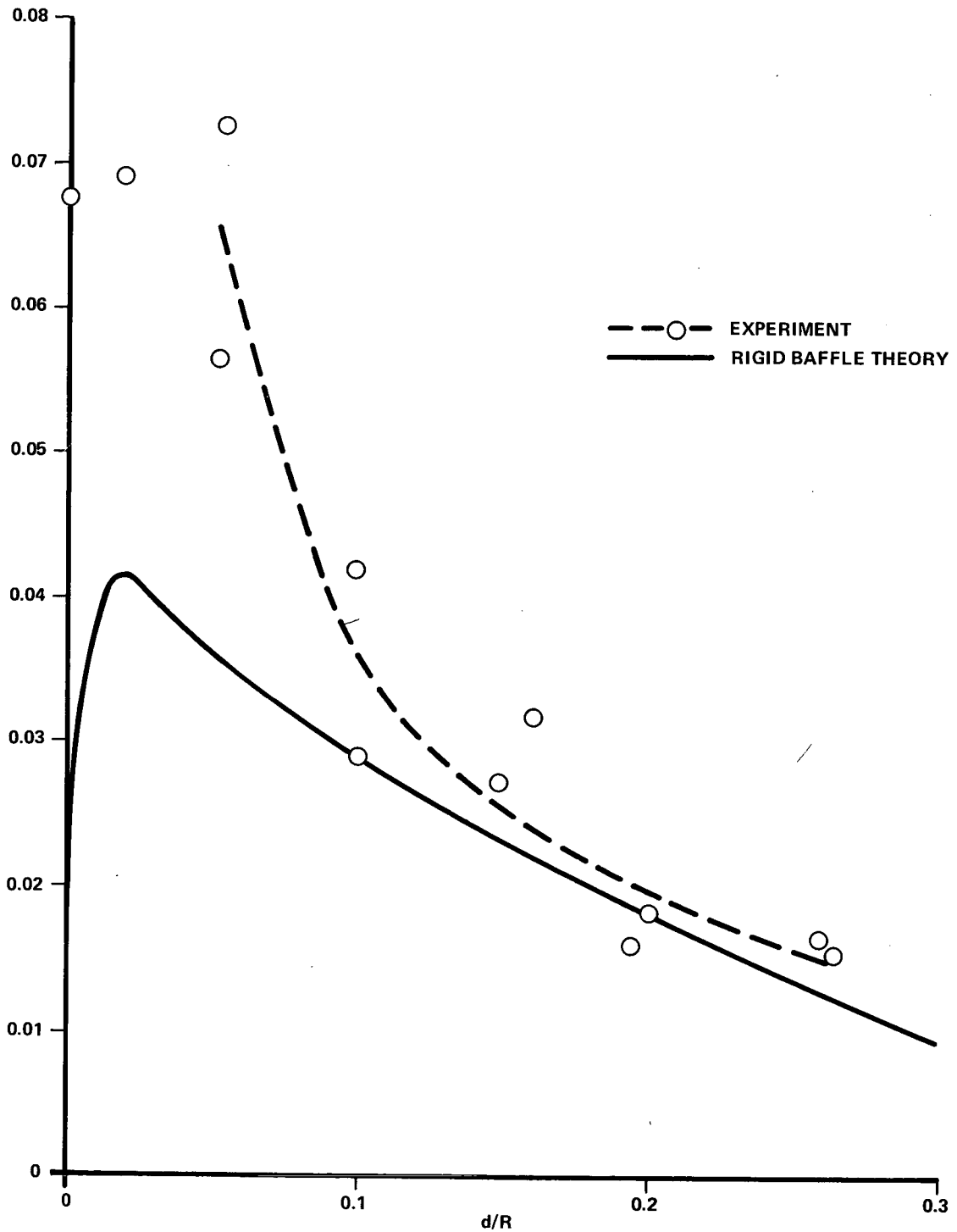
Figure 8b,  $\zeta/R = 0.04$ , shows the same trend of damping versus baffle depth as seen at  $\zeta/R = 0.02$ , but the damping advantage of the flexible baffle over the rigid baffle is smaller. In Figure 8c,  $\zeta/R = 0.06$ , there is considerable data scatter. The flexible baffle damping appears to be approximately equal to the rigid baffle damping through the range of baffle depths investigated.

Figure 9 shows the damping provided by the flexible Teflon baffle as a function of baffle depth. Figure 9a,  $\zeta/R = 0.02$ , shows the Teflon baffle damping as considerably higher than rigid baffle damping for baffle depths between  $d/R = 0$  and about 0.15. For the other depths and amplitudes shown in Figures 9b and 9c, the flexible and rigid baffle damping are approximately equal.

Effect of Amplitude. Figure 10 shows damping as a function of amplitude at three baffle depths for the steel and Teflon baffles and compares this with rigid baffle theory [equation (3)]. The experimental data presented in Figure 10 were taken from the dashed curves in Figures 8 and 9.

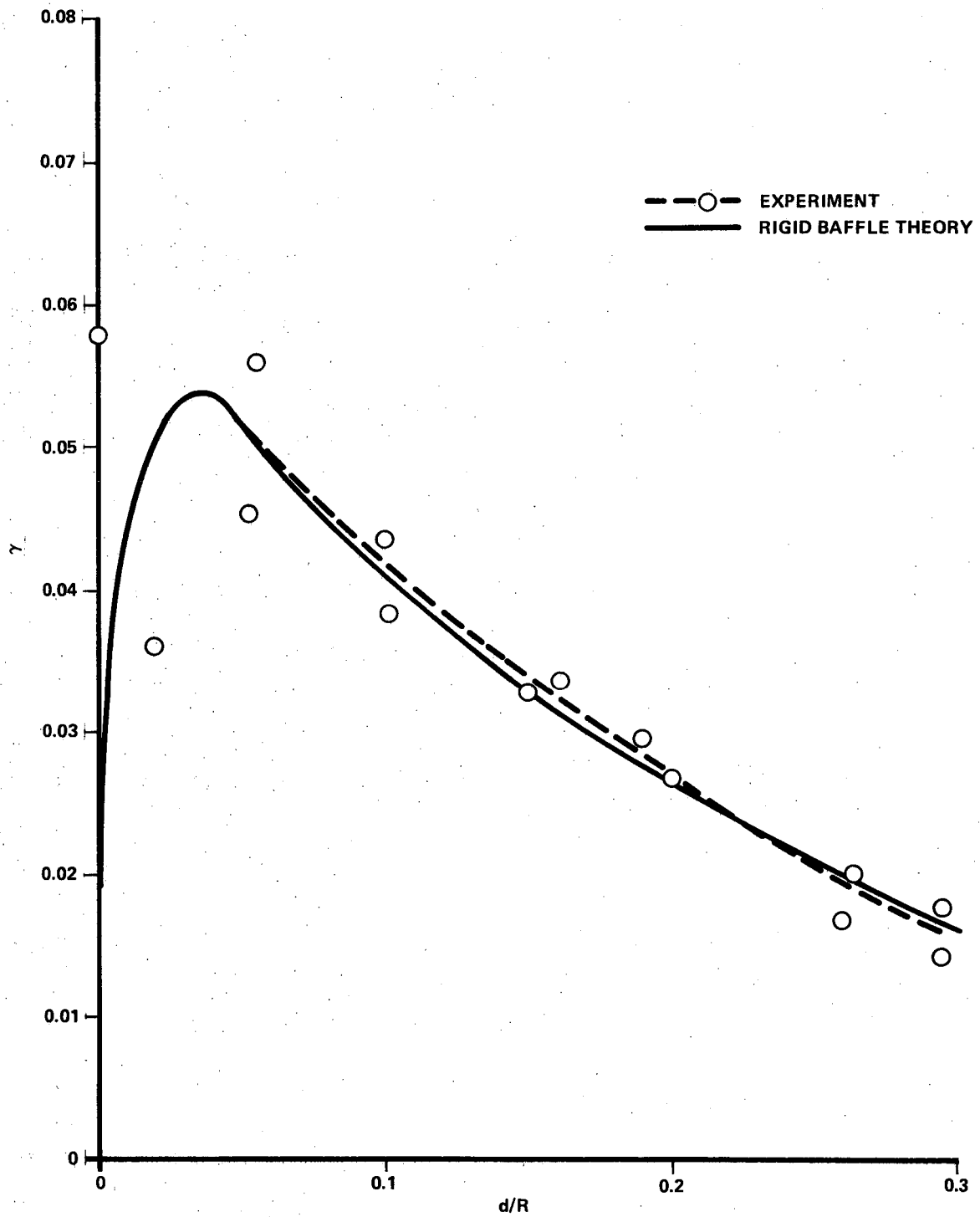
TABLE 2. CALCULATED DATA

Baffle	$\frac{d}{R}$	$\gamma_r$ ( $\frac{L}{R} = 0.02$ )	$\gamma_r$ ( $\frac{L}{R} = 0.04$ )	$\gamma_r$ ( $\frac{L}{R} = 0.06$ )	P ( $\frac{L}{R} = 0.02$ )	P ( $\frac{L}{R} = 0.04$ )	P ( $\frac{L}{R} = 0.06$ )	F	$\frac{\gamma_f}{\gamma_r}$ ( $\frac{L}{R} = 0.02$ )	$\frac{\gamma_f}{\gamma_r}$ ( $\frac{L}{R} = 0.04$ )	$\frac{\gamma_f}{\gamma_r}$ ( $\frac{L}{R} = 0.06$ )
Steel	0	0.016	0.0225	0.0277	1.00	2.01	3.01	0.538	2.90	2.18	1.80
	0.0154	0.041	0.0484	0.0521	0.97	1.95	2.92		2.18	0.66	0.82
	0.0487	0.0366	0.0516	0.0613	0.91	1.83	2.74		1.61	1.15	--
	0.0628	0.0344	0.0478	0.0582	0.89	1.78	2.66		1.71	1.24	--
	0.1101	0.0282	0.0389	0.0470	0.82	1.63	2.44		1.35	1.13	1.05
	0.1129	0.0280	0.0382	0.0463	0.81	1.63	2.43		1.46	1.08	1.29
	0.1475	0.0232	0.0331	0.0401	0.76	1.53	2.28		1.23	1.10	1.07
	0.150	0.0230	0.0329	0.0396	0.76	1.51	2.27		1.47	1.04	0.87
	0.203	0.0179	0.0261	0.0316	0.69	1.37	2.05		1.31	0.92	0.81
	0.205	0.0176	0.0259	0.0315	0.69	1.37	2.05		1.68	1.16	--
	0.214	0.0168	0.0250	0.0303	0.67	1.35	2.01		1.39	1.16	1.22
	0.251	0.0135	0.0210	0.0258	0.63	1.25	1.88		1.41	1.00	--
	0.259	0.0129	0.0201	0.0259	0.62	1.23	1.85		1.50	1.01	--
	0.304	0.0092	0.0156	0.0200	0.57	1.14	1.71		1.47	1.12	1.12
	0.307	0.0090	0.0152	0.0197	0.56	1.14	1.69		--	1.01	1.32
Teflon	0	0.016	0.0225	0.0277	1.00	2.01	3.01	0.245	4.22	2.57	1.90
	0.018	0.0412	0.0502	0.0539	0.97	1.94	2.91		1.67	0.72	0.96
	0.0513	0.0361	0.0503	0.0607	0.90	1.82	2.73		1.56	0.90	--
	0.0538	0.0358	0.0502	0.0605	0.90	1.81	2.71		2.03	1.12	--
	0.0987	0.0293	0.0410	0.0494	0.83	1.66	2.49		1.43	1.06	0.95
	0.100	0.0290	0.0407	0.0492	0.83	1.66	2.49		1.00	0.94	--
	0.148	0.0232	0.0330	0.0400	0.76	1.52	2.28		1.17	0.99	0.93
	0.160	0.0220	0.0315	0.0380	0.74	1.49	2.23		1.44	1.07	0.94
	0.188	0.0191	0.0277	0.0337	0.70	1.41	2.11		0.83	1.07	1.28
	0.199	0.0181	0.0265	0.0321	0.69	1.38	2.07		1.02	1.01	1.13
	0.259	0.0128	0.0201	0.0249	0.62	1.23	1.85		1.28	0.83	1.34
	0.263	0.0126	0.0194	0.0244	0.61	1.22	1.84		1.21	1.03	--
	0.294	0.0100	0.0165	0.0210	0.58	1.15	1.74		--	1.07	--
	0.294	0.0100	0.0165	0.0210	0.58	1.15	1.74		--	0.86	0.84



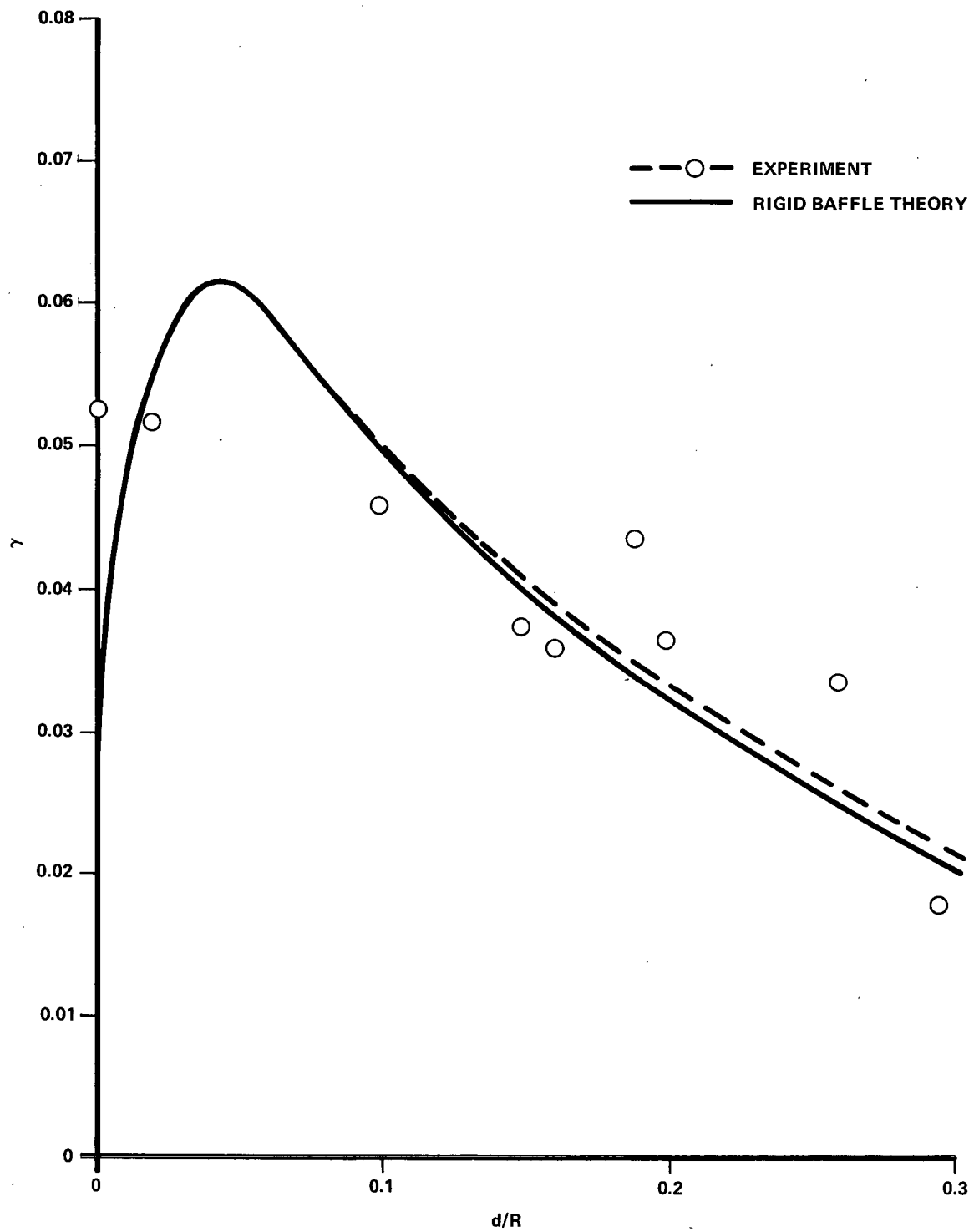
(a).  $\zeta/R = 0.02$ .

Figure 9. Effect of Teflon baffle depth on damping.



(b).  $\zeta/R = 0.04$ .

Figure 9. (Continued).



(c).  $\zeta/R = 0.06$ .

Figure 9. (Concluded).

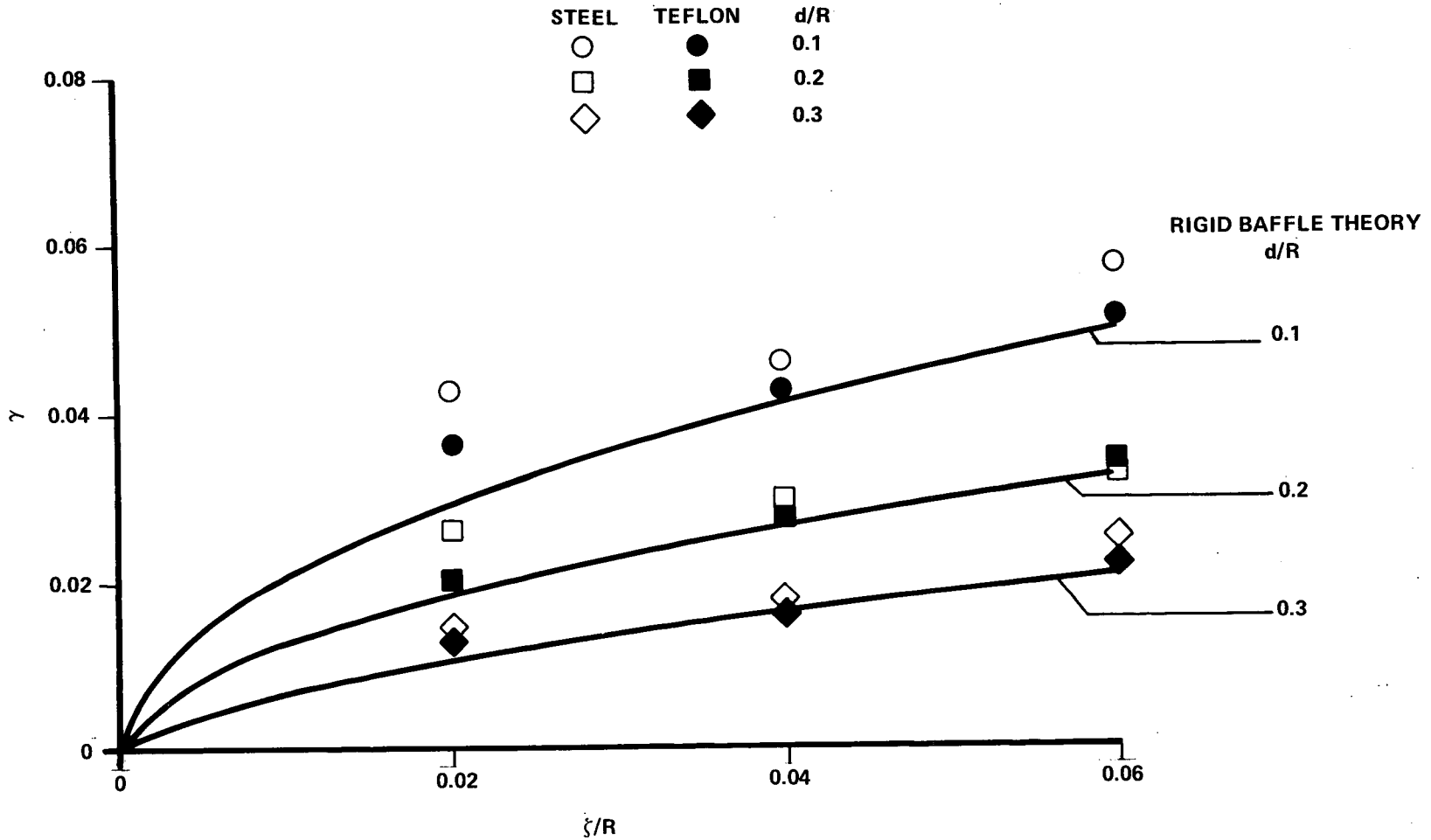


Figure 10. Effect of slosh amplitude on damping.

The flexible baffle damping is seen to increase similarly to rigid baffle damping as the amplitude increases. The damping advantage of flexible over rigid baffles appears greater at low amplitude. The steel baffle produced an average of 42 percent more damping than rigid at  $\zeta/R = 0.02$  and an average of 12 percent more than the rigid baffle at  $\zeta/R = 0.06$ .

Period Parameter and Flexibility Parameter. Reference 2 shows that two important dimensionless ratios which affect flexible baffle damping are the period parameter, proportional to the ratio of liquid amplitude to baffle width, and the flexibility parameter, proportional to the ratio of baffle deflection to baffle width. The period parameter is computed by the formula

$$P = \frac{2\pi\zeta}{W} e^{-1.84 \left(\frac{d}{R}\right)}$$

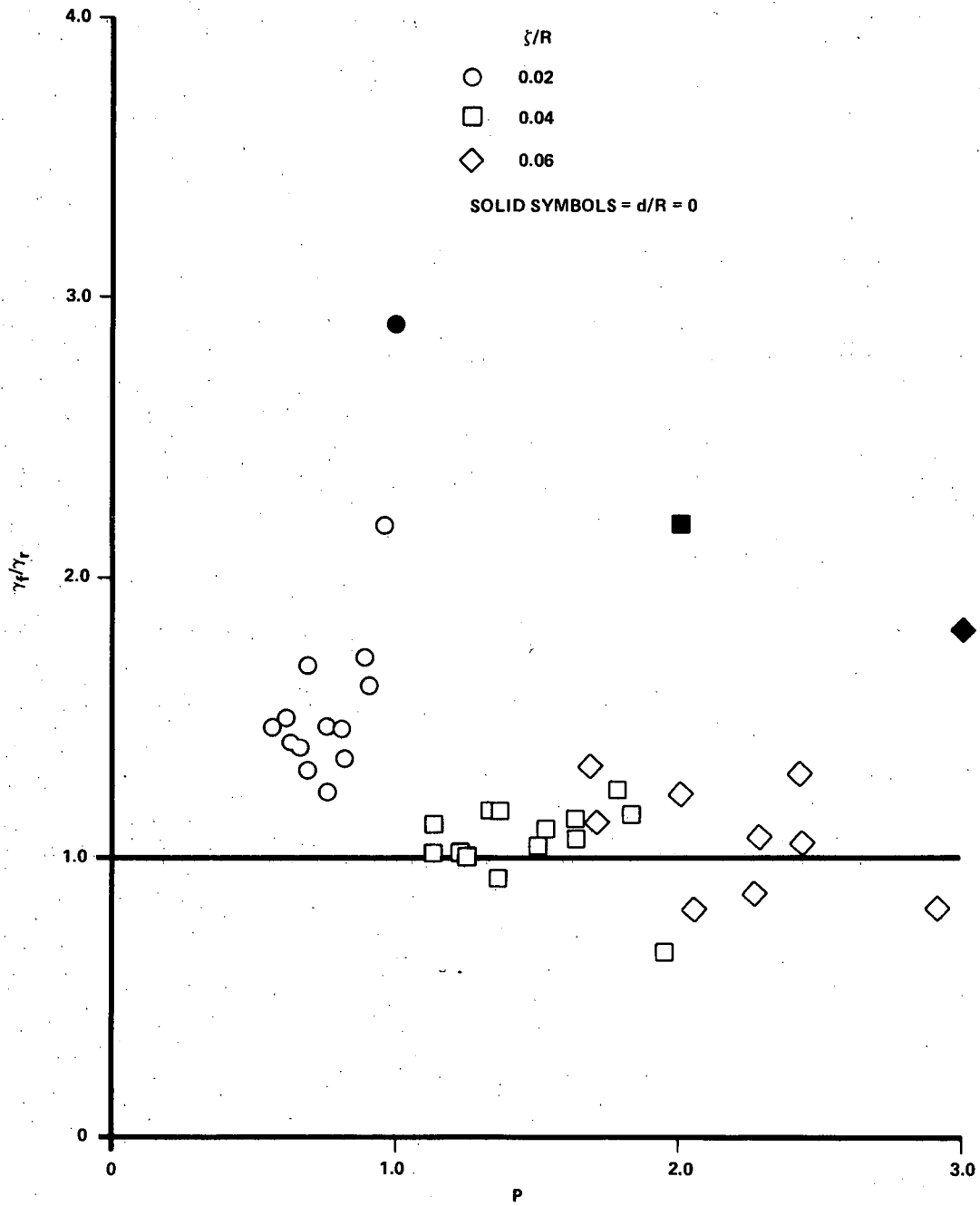
and the flexibility parameter by

$$F = 0.04 \left(\frac{\rho g R}{E}\right) \left(\frac{W_f}{R}\right)^5 \left(\frac{R}{t}\right)^3,$$

both taken from Reference 4.

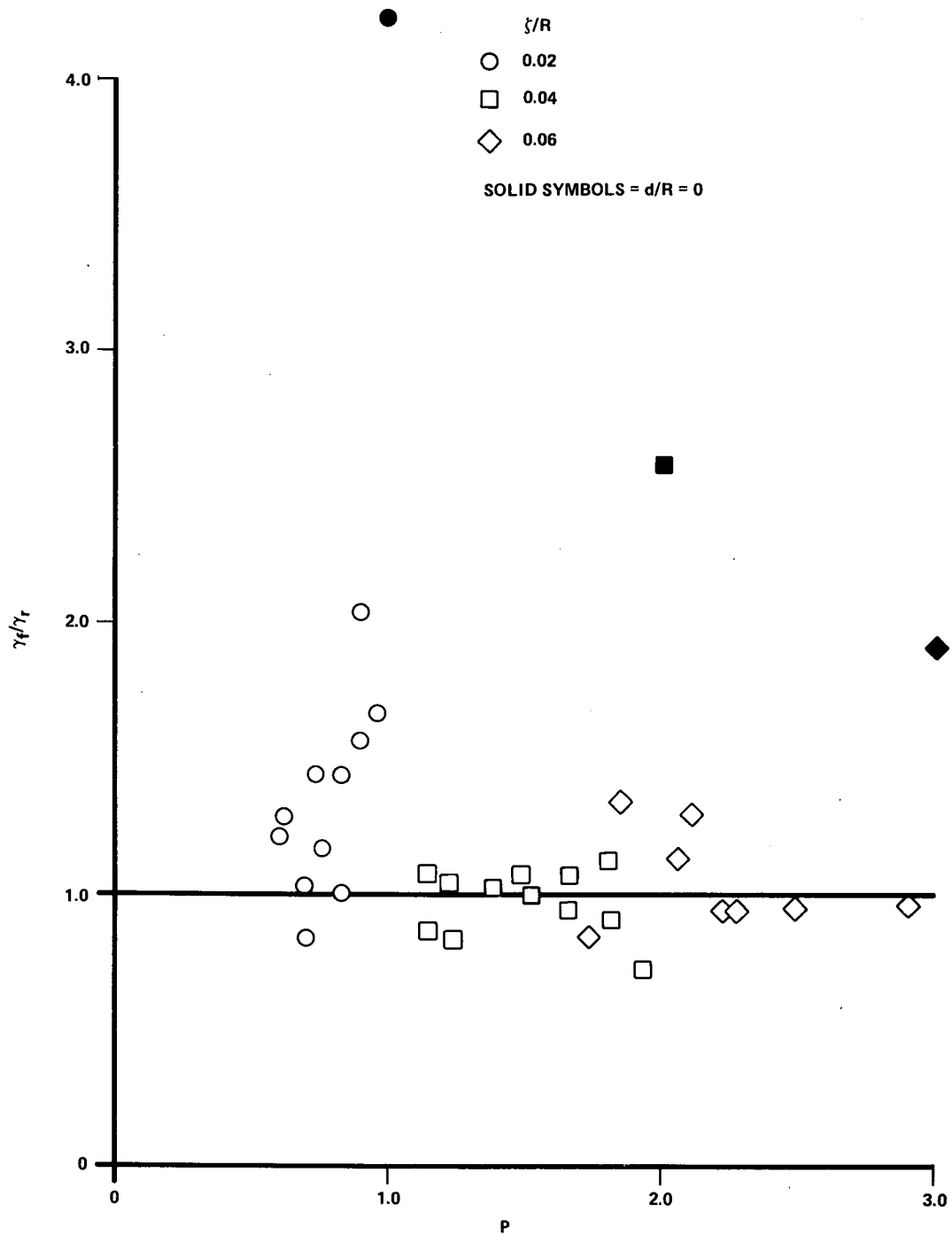
Figure 11 shows the relationship between the period parameter,  $P$ , and the ratio of flexible to rigid baffle damping. The values of  $P$  and  $\gamma_f/\gamma_r$  are also shown in Table 2. For baffle depths greater than  $d/R = 0$ , the relative damping was found to be independent of depth and showed a slight decrease with increasing  $P$  for both steel and Teflon baffles. Amplitudes seen during Saturn V flights were usually  $0.03 R$  or less, which would give values less than 1.2 for  $P$ . The propellant drop tank of the proposed Space Shuttle orbiter should also experience slosh amplitudes which give  $P = 1.2$  or less during the majority of boost flight time. The highest values  $\gamma_f/\gamma_r$  in Figure 11 are seen to be in this practical period parameter range.

The flexibility parameter,  $F$ , was 0.245 for the Teflon baffle and 0.538 for the steel baffle. The effective flexibility was probably greater than this due to the slight droop of these baffles as installed. Both of these were more flexible than any of the baffles tested in Reference 2 where the largest flexibility was  $F = 0.203$ . The change in  $\gamma_f/\gamma_r$  with flexibility seen in the present investigation agrees with the trends reported in Reference 2; that is, the more flexible steel baffle ( $F = 0.538$ ) produced slightly higher values of  $\gamma_f/\gamma_r$  than the Teflon baffle ( $F = 0.245$ ) for values of  $P$  below about 1.5 and for baffle depths greater than 0.



(a). Steel baffle.

Figure 11. Effect of period parameter on relative damping.



(b). Teflon baffle.

Figure 11. (Concluded).

## Strength and Weight

The steel baffle was subjected to approximately 300 cycles of liquid oscillation during the test (less than 200 cycles are expected per Space Shuttle flight in the propellant drop tanks being considered). The highest stress conditions gave a factor of safety of 2.0, calculated using equations (1) and (2). Since Reference 4 recommended  $K = 3$  for use in equation (1), the steel baffle was stressed 50 percent beyond the recommended value. After completion of the test program, the steel baffle was examined and found to be intact with no signs of failure.

The Teflon baffle was tested in a similar program and went through approximately 280 liquid-oscillation cycles. The lowest safety factor during the basic test program was 2.5 (20 percent greater stress than recommended). After completion of the basic program, the Teflon baffle was tested at an amplitude which gave a safety factor of 0.78 (i.e., the stress in the baffle calculated by equations (1) and (2) was 28 percent more than the Teflon yield strength). The baffle failed, as expected, during excitation of the liquid such that the damping during free decay was very low, approximately = 0.015. Examination of the broken baffle showed primarily radial breaks in the Teflon. The only portions of the baffle that remained intact were two segments at each liquid oscillation node.

Based on the results above, it appears that equations (1) and (2) are adequate for baffle thickness determination when used with a safety factor of 3, as suggested in Reference 4.

Reference 4 showed the weight of a flexible baffle to be proportional to the parameter  $\left(\rho_B E^{\frac{1}{2}}\right) / \left(\sigma_y^{3/2}\right)$ . Values of this weight parameter for the two materials of the present investigation and two other materials are shown below:

Material	$\rho_B$ , gm/cm <sup>3</sup>	$\sigma_y$ , $\frac{\text{dynes}}{\text{cm}^2}$	E, $\frac{\text{dynes}}{\text{cm}^2}$	$\frac{\rho_B E^{\frac{1}{2}}}{\sigma_y^{3/2}}$ , $\frac{\text{sec}^2}{\text{cm}^2}$
Type 301 stainless steel	7.85	$100.8 \times 10^8$	$207 \times 10^{10}$	$11.16 \times 10^{-9}$
Teflon FEP	2.15	$8.86 \times 10^8$	$7.2 \times 10^{10}$	$21.88 \times 10^{-9}$
Type 301 stainless steel	7.85	$220.6 \times 10^8$	$207 \times 10^{10}$	$3.45 \times 10^{-9}$
7075 aluminum	2.80	$49.6 \times 10^8$	$68.95 \times 10^{10}$	$6.65 \times 10^{-9}$

Type 301 stainless steel is available with various yield strengths depending on the cold-work process applied. The steel and Teflon properties are from Reference 5, and the aluminum properties are from Reference 7. The lightest of the six plastic baffle materials studied in Reference 4 had values of  $\left(\rho_B E^{\frac{1}{2}}\right) / \left(\sigma_y^{3/2}\right)$  near  $6.0 \times 10^{-9} \text{ sec}^2/\text{cm}^2$ . The high strength stainless steel appears to be the best choice of flexible material of those studied in References 4 and 5 and the present investigation based on weight and oxygen compatibility.

## CONCLUSIONS

An experimental investigation was made of damping produced by single flexible ring baffles in a 396-cm diameter tank of liquid nitrogen. Two baffles were tested. Each baffle was 24.8-cm wide. One baffle was 0.00635-cm thick type 301 stainless steel and the other was 0.0254-cm thick Teflon FEP. Each baffle produced damping of liquid oscillations equal to or greater than that expected from rigid baffles at all test conditions. The maximum damping recorded was 8.9 percent of critical, produced by the steel baffle at a baffle depth equal to 0.0154 times the tank radius with a liquid oscillation amplitude of 0.02 times the tank radius. This damping value was 2.18 times the damping expected from a rigid baffle for the same conditions.

The design equations with their accompanying safety factor recommendations were found to be adequate for determination of flexible baffle thickness required. The steel baffle was stressed 50 percent greater than recommended and the Teflon baffle 20 percent greater than recommended without failure. For the same application, a lighter weight baffle could be constructed using stainless steel rather than using Teflon.

## REFERENCES

1. Silveira, Milton A.; Stephens, David G.; and Leonard, H. Wayne: "An Experimental Investigation of the Damping of Liquid Oscillations in Cylindrical Tanks with Various Baffles," NASA TN D-714, May 1961.
2. Stephens, David G.; and Scholl, Harland F.: "Effectiveness of Flexible and Rigid Ring Baffles for Damping Liquid Oscillations in Large-Scale Cylindrical Tanks," NASA TN D-3878, 1967.
3. Garza, Luis R.: "A Comparison of Flexible and Rigid Ring Baffles for Slosh Suppression," SwRI Project No. 02-1846, Report No. 1, August 1966.
4. Dodge, Franklin T.: "Engineering Study of Flexible Baffles for Slosh Suppression," SwRI Project 02-2841, Final Report, 1970.
5. Bass, R. L.: "Stress-Corrosion and Fatigue Testing of Flexible Baffle Materials," SwRI Project No. 02-3243 Final Report, February 1972.
6. Abramson, H. N.: "The Dynamic Behavior of Liquids in Moving Containers," NASA SP-106, 1966.
7. Marks Mechanical Engineers Handbook, Theodore Baumeister, Editor, Sixth Edition, McGraw-Hill Book Company, Inc., 1958.

## APPROVAL

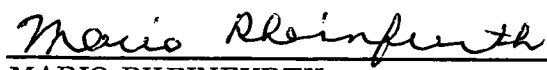
# EVALUATION OF FLEXIBLE RING BAFFLES FOR DAMPING LIQUID OSCILLATIONS

By Frank Bugg

The information in this report has been reviewed for security classification. Review of any information concerning Department of Defense or Atomic Energy Commission programs has been made by the MSFC Security Classification Officer. This report, in its entirety, has been determined to be unclassified.

This document has also been reviewed and approved for technical accuracy.

  
\_\_\_\_\_  
LARRY A. KIEFLING  
Chief, Structural Dynamics Section

  
\_\_\_\_\_  
MARIO RHEINFURTH  
Chief, Dynamics Analysis Branch

  
\_\_\_\_\_  
J. A. LOVINGOOD  
Chief, Dynamics and Control Division

  
\_\_\_\_\_  
E. D. GEISLER  
Director, Aero-Astrodynamic Laboratory

# DISTRIBUTION

## INTERNAL

DIR

DEP-T

A&PS-PAT

A&PS-MS-H

A&PS-MS-IP (2)

A&PS-MS-IL (8)

A&PS-TU

Mr. Wiggins (6)

S&E-ASTN

Mr. Heimburg

Mr. Sterett

Mr. Connor

Mr. Goetz

Mr. Funkhouser

Mr. Jones

Mr. Linnan

S&E-ASTR

Mr. Moore

Mr. Mink

S&E-AERO

Dr. Geissler

Mr. Horn

Mr. Sims

Mr. Jackson

Mr. McAnnally

Dr. Lovingood

Mr. Ryan

Mr. Rheinfurth

Mr. Kiefling

Mr. Mowery

Mr. Sugg (15)

## EXTERNAL

Scientific & Technical Information Facility (2)

P.O. Box 33

College Park, Md. 20740

ATTN: NASA Rep. (S-AK/RKT)

Mr. Grady Riley

The Boeing Company

P.O. Box 1470

Huntsville, Alabama 35807

E. Lerner

Grumman Aerospace Corp.

Structural Mechanics -

Plant 35

Bethpage, New York 11714

Roger Gieseke

Convair Division, General Dynamics

P.O. Box 1128

San Diego, Calif. 92112

Lee Olson

McDonnell-Douglas Corp.

5301 Bolsa Avenue

Huntington Beach, Calif. 92647

George Morosow

Martin-Marietta Corp.

Denver Division

P.O. Box 179

Denver, Colorado 80201

Tom Modlin

ES-2

NASA, Manned Spacecraft

Center

Houston, Texas 77058

Walter J. Mykytow

Vehicle Dynamics Division

USAF Flight Dynamics

Laboratory

Wright-Patterson AFB

Dayton, Ohio 45433

Dr. Helmut F. Bauer

School of Engineering Science and Mechanics

Georgia Institute of Technology

Atlanta, Georgia 30332

C.M. Pearson

Northrop Corporation

P.O. Box 1484

Huntsville, Alabama 35805

Gunter Schurr, AB-18

North American Rockwell Corp.

12214 Lakewood Blvd.

Downey, Calif. 90241

Manned Spacecraft Center

Houston, Texas

ATTN: Mr. Robert F. Thompson

Code LA

Mr. Milton Silveira,

Code EA-9

Langley Research Center

Langley Station

Hampton, Va. 23365

ATTN: Mr. Stephens, MS 230

Mr. Eide, MS 163-A

Dr. W.A. McNeill

Engineering Division

University of South Alabama

Mobile, Alabama 36608

Mr. Douglas Michel

RV-2

NASA

Washington, D.C.

W.D. Whetstone

Lockheed HREC

P.O. Box 1103

West Station

Huntsville, Alabama

Dr. Norman Abramson

P.O. Drawer 28510

Southwest Research

Institute

San Antonio, Texas 78228

Roger Barnes

Convair Division, General

Dynamics

P.O. Box 80847

San Diego, Calif. 92138

Ed Lamb

M.S. LLOO

The Boeing Company

Michoud, Louisiana 70129

Kenneth S. Kaye

Chrysler Corporation

Michoud, Louisiana 70129

James T. McPherson

McDonnell-Douglas Corp.

Structural Dynamics Dept.

E236

P.O. Box 516

St. Louis, Missouri 63166

Theodore F. Gerus

Code 500-119

NASA/Lewis Research Center

21000 Brookpark Road

Cleveland, Ohio 44135

Dr. E.R. Fleming

Aerospace Corp.

2400 E. El Segundo Blvd.

El Segundo, Calif. 90245